Reaction of Modified and Unmodified $tRNA^{Tyr}$ Substrates with Tyrosyl-tRNA Synthetase (*Bacillus stearothermophilus*)†

Johanna M. Avis,‡ Anthony G. Day, George A. Garcia,§ and Alan R. Fersht*

Medical Research Council Unit for Protein Function and Design, Department of Chemistry, University of Cambridge, Lensfield Road, Cambridge CB2 1EW, United Kingdom

Received November 19, 1992; Revised Manuscript Received February 15, 1993

ABSTRACT: Three species of $tRNA^{Tyr}$ have been examined as substrates for the transfer reaction of the tyrosyl-tRNA synthetase (TyrRS) from *Bacillus stearothermophilus*: *Escherichia coli* $tRNA^{Tyr}$, *B. stearothermophilus* $tRNA^{Tyr}$ expressed in *E. coli*, and *B. stearothermophilus* $tRNA^{Tyr}$ that has been transcribed in vitro. The binding of the first two substrates to TyrRS may be readily monitored by stopped-flow studies of tryptophan fluorescence to give the rate and equilibrium constants. The in vitro-transcribed $tRNA^{Tyr}$, which lacks the modified bases queuosine and 2-(methylthio)-N^6-isopentenyladenosine in the anticodon loop, does not cause a significant change in tryptophan fluorescence upon binding. The three $tRNA^{Tyr}$ substrates exhibit very similar steady-state kinetics in the charging reaction. Pre-steady-state kinetics of the transfer reaction, monitored by stopped-flow measurements of the change in protein fluorescence on the addition of $tRNA^{Tyr}$ to the E·Tyr-AMP complex, show two exponential changes for the modified $tRNA^{Tyr}$ substrates. The first is that due to substrate binding. The second has an identical rate to the single change observed for the reaction with the in vitro-transcribed $tRNA^{Tyr}$ and to that monitored by quenched-flow measurements on the formation of Tyr-$tRNA^{Tyr}$. Hence, the transfer reaction can be observed by stopped-flow. The dissociation constants (K_{tRNA}) of tRNA from the enzyme and rates of tyrosine transfer (k_4) show that all three tRNA molecules are kinetically equivalent substrates for TyrRS. The value of k_4 is also similar to that found for authentic $tRNA^{Tyr}$ from *B. stearothermophilus*. The in vitro-transcribed $tRNA^{Tyr}$, which can be isolated in large quantities, is a suitable substrate for extended studies of the transfer reaction monitored by stopped-flow fluorescence. The free energies of two further species on the TyrRS reaction pathway, the complex with bound $tRNA^{Tyr}$ and the subsequent transition state of tyrosine transfer, can now be calculated. The free energies of activation of the two chemical steps on the reaction pathway, activation and transfer, are of equal magnitude (15.4 kcal mol^{-1}). The optimization of overall catalysis during evolution has presumably involved selective pressure on both steps.

The tyrosyl-tRNA synthetase from *Bacillus stearothermophilus* (TyrRS)[1] is a dimeric enzyme of M_r 2 × 47 316 which belongs to the class I synthetases that are characterized by possessing the Rossman nucleotide binding fold (Rossman et al., 1974). The enzyme catalyzes the aminoacylation of tRNA in a two-step reaction:

$$E + Tyr + Mg{\cdot}ATP \rightleftarrows E{\cdot}Tyr\text{-}AMP + Mg{\cdot}PP_i \quad (1)$$

$$E{\cdot}Tyr\text{-}AMP + tRNA^{Tyr} \rightleftarrows E{\cdot}Tyr\text{-}tRNA^{Tyr} + AMP \quad (2)$$

A combination of X-ray crystallography (Brick et al., 1989), protein engineering (Winter et al., 1982), and steady-state and pre-steady-state kinetics has led to the elucidation of the mechanism of step I, tyrosyl adenylate formation (Fersht, 1987). Pre-steady-state kinetics was essential for construction of accurate free energy profiles for the reactions catalyzed by wild-type and mutant enzymes. There is little detailed information on step II; X-ray crystallographic information concerning the TyrRS–$tRNA^{Tyr}$ interaction is not available at present, and the simple steady-state tRNA charging assays that have previously been employed cannot isolate step II from step I. The application of pre-steady-state kinetic techniques, with the aim of isolating reaction intermediates on the tRNA charging step and their associated equilibrium and rate constants, is necessary for completing the kinetic analysis of the overall pathway and mechanism of the reaction. The tyrosyl adenylate complex that is formed as a reaction intermediate in step I is extremely stable and can be isolated and then mixed with $tRNA^{Tyr}$ to observe step II of the enzyme reaction. The major problem in applying pre-steady-state kinetics has been the difficulty of obtaining large supplies of pure tRNA. In this study, we have compared the cognate *B. stearothermophilus* $tRNA^{Tyr}$, expressed in *Escherichia coli*, with the more readily available *E. coli* $tRNA^{Tyr}$ and a *B. stearothermophilus* $tRNA^{Tyr}$ substrate lacking base modifications, obtained in high yields from in vitro transcription.

In the process, we have gathered information on whether the bacterial source of the $tRNA^{Tyr}$ affects the TyrRS tRNA charging kinetics and whether the base modifications present in the natural $tRNA^{Tyr}$ substrate are important for specific recognition by TyrRS. The enzymes from the two species share 56% identity (Barker et al., 1982; Jones et al., 1986). Their $tRNA^{Tyr}$ substrates share 72% identity, 27% resulting

† J.M.A. was supported by a Science and Engineering Research Council Studentship.

‡ Present address: Laboratory of Molecular Biology, Medical Research Centre, Hills Road, Cambridge CB2 2QH, U.K.

§ Present address: College of Pharmacy, University of Michigan, 428 Church St., Ann Arbor, Michigan 48109-1065.

[1] Abbreviations: aaRS, aminoacyl-tRNA synthetase; TyrRS, tyrosyl-tRNA synthetase; XxxNn, mutant tyrosyl-tRNA synthetase with amino acid Xxx at position Nn; Tyr (T), tyrosine; Tyr-AMP (T-A), tyrosyl adenylate; Tyr-tRNA, tyrosine attached to 3′ terminus of tRNA; RNasin, placental ribonuclease inhibitor; Tris, 2-amino-2-(hydroxymethyl)-1,3-propanediol; PP_i, inorganic pyrophosphate; DTT, dithiothreitol; EDTA, ethylenediaminetetraacetic acid; FPLC, fast protein liquid chromatography; PMSF, phenylmethanesulfonyl fluoride; TY, tryptone–yeast; TCA, trichloroacetic acid.

0006-2960/93/0432-5312$04.00/0

from bases that are invariant or semi-invariant among all tRNAs (Sprinzl & Gauss, 1982). Many aminoacyl-tRNA synthetase–tRNA interactions have been investigated using RNA substrates that have been transcribed in vitro and lack the characteristic base modifications present in the natural substrates. For the majority of cases where a comparison has been made, the modified and unmodified tRNA substrates exhibit identical steady-state charging kinetics. Modified bases in these cases are possibly more important for the subsequent interactions between the tRNA molecule and the translational apparatus (Bjork et al., 1987). Recent work, however, has shown that unmodified $tRNA^{Asp}$ transcripts possess a relaxed conformation in solution compared with that of native yeast $tRNA^{Asp}$ (Perret et al., 1990), suggesting the base modifications are stablizing the biologically active conformation of the tRNAs. NMR studies have shown that unmodified yeast $tRNA^{Phe}$ folds normally and attains full aminoacylation activity only when the Mg^{2+} concentration is high (Hall et al., 1989). In the case of an *E. coli* $tRNA^{Ile}$ isoacceptor, the lysidine in the anticodon is essential for aminoacylation (Maramatsu et al., 1988).

MATERIALS AND METHODS

Materials. DNA restriction endonucleases, T4 polynucleotide kinase, and T4 DNA ligase were from New England Biolabs. Placental ribonuclease inhibitor (RNasin) was purchased from Promega. Oligonucleotides were produced on an automated DNA synthesizer (Applied Biosystems Inc., Model 380B). T7 RNA polymerase was isolated from pAR1219/*E. coli* BL21 by a modification of the procedure of Grodberg and Dunn (1988). After ammonium sulfate precipitation, the sample was dialyzed against 1 L of 20 mM $NaHPO_4/Na_2PO_4$ (pH 7.7), 1 mM EDTA, 1 mM dithiothreitol, 0.1 mM PMSF, 25 mM NaCl, and 5% glycerol. The sample was purified by anion-exchange chromatography on FPLC Mono Q with a gradient of 25–500 mM NaCl in the dialysis buffer. The final sample was 120 000 units/mg and 1 mg/mL = 1.3 A_{280}. Uniformly-labeled [^{14}C]tyrosine (486 mCi/mmol) was purchased from Amersham International. Nitrocellulose discs (Type 11306) were obtained from Sartorius.

Preparation of TyrRS. The tyrosyl-tRNA synthetase from *B. stearothermophilus* was expressed in *E. coli* TG2 cells under the control of the inducible *tac* promoter in pYTS5 and purified according to E. A. First (unpublished). TyrRS concentration was determined by active-site titration as described elsewhere (Wilkinson et al., 1983).

$tRNA^{Tyr}$ Substrates. In the preparation, storage, and incubation of $tRNA^{Tyr}$ substrates, all buffers are pretreated with diethyl pyrocarbonate (Sigma) as a precaution against ribonucleases. *E. coli* $tRNA^{Tyr}$ was purchased from Subriden RNA and its concentration was determined on the basis of tyrosine acceptance (1000 pmol/A_{260}).

Expression of B. stearothermophilus $tRNA^{Tyr}$ in E. coli. A plasmid, pTB9, containing the *B. stearothermophilus* $tRNA^{Tyr}$ gene had been previously constructed by T. Borgford (unpublished). The gene was replicated from this construct using the polymerase chain reaction (Saiki et al., 1988) and subcloned into pKK223-3 downstream of the inducible *tac* promoter. The correct tRNA gene sequence was verified by double-stranded DNA sequencing using the Sequenase protocol provided by U.S. Biochemical Corp. The construct, pJA1, was transformed into the ribonuclease-deficient *E. coli* strain MRE 600. An overnight culture of pJA1/MRE in 2× TY medium with 50 μg/mL ampicillin was diluted 100-fold into 100 mL of fresh medium and the cells were grown at 37 °C to an A_{600} of 0.6, at which stage the culture was used to inoculate 10 L of medium. The *tac* promoter was induced by addition of IPTG to 0.15 mM when the culture had reached an A_{600} of 1.0. The cells were grown a further 6 h and then harvested by centrifugation. The pellets were immediately resuspended in 100–150 mL of a denaturing/lysis buffer consisting of 4 M guanidinium thiocyanate, 25 mM sodium citrate (pH 7), 0.5% sarcosyl, and 0.1 M 2-mercaptoethanol. The acid guanidinium thiocyanate–phenol–chloroform method of cell lysis and ribonucleic acid extraction was used (Chomczynski & Sacchi, 1987). After extraction, the aqueous layer was saved and precipitated with an equal volume of 2-propanol. The whole extraction and precipitation process was repeated twice, after which the precipitate was washed with 70% ethanol, resuspended in 4 M LiCl, and incubated at −20 °C for 2 h. Precipitate was removed by centrifugation. The tRNA was precipitated from the supernatant with an equal volume of 2-propanol at −20 °C. The precipitate was washed with 70% ethanol and resuspended in 50 mL of 10 mM sodium acetate (pH 5.0) and 10 mM $MgCl_2$ for batch elution from BND-cellulose (Sigma). The sample was bound to 60 g of BND-cellulose for 2 h. The cellulose was washed twice with more of the same buffer and then washed with 10 mM sodium acetate (pH 5.0), 10 mM $MgCl_2$, 1 M NaCl, and 20% ethanol to remove the $tRNA^{Tyr}$. This sample was 2-propanol-precipitated. The precipitate was resuspended in 10 mM sodium acetate (pH 4.5), 10 mM $MgCl_2$, and 0.2 M NaCl and fractionated with a 0.2–1.0 M NaCl gradient on NACS-20 resin (Bethesda Research Laboratories, Inc.) which was packed into a Pharmacia HR16/10 FPLC column. There were two peaks corresponding to $tRNA^{Tyr}$, one of much higher purity than the other (measured in terms of picomoles per milliliter of [^{14}C]tyrosine acceptance per A_{260} unit). The tRNA present in greater quantity and higher purity is the overexpressed *B. stearothermophilus* $tRNA^{Tyr}$. The sample was precipitated, resuspended, and repassed through the NACS-20 column to reach a final purity of 850–1000 pmol/A_{260} (i.e., 80–90% pure). The final yield was 2–5 mg.

In Vitro Transcription of B. stearothermophilus $tRNA^{Tyr}$. The gene was excised from the polylinker of pTB9 by digestion with *Eco*RI and *Pst*I restriction endonucleases and inserted into the polylinker of pTZ18U (immediately downstream of the T7 promoter). The *Pst*I site was changed to a *Bst*NI site by mutagenesis according to the protocols in the Amersham mutagenesis kit. The *Bst*NI site was immediately downstream of the tRNA gene. This construct, pGAG2, was digested with *Bst*NI and used in transcription reactions. A typical 5-mL reaction contained 40 mM Tris-HCl (pH 8.1 at 37 °C), 6 mM $MgCl_2$, 5 mM DTT, 2 mM spermidine, 50 μg/mL bovine serum albumin, 1200 units of RNasin, 2 units of pyrophosphatase, 100 μL of T7 RNA polymerase, 4 mM each NTP, and 100 μg of *Bst*NI-linearized pGAG2. After incubation at 37 °C for 4–5 h, the $tRNA^{Tyr}$ was extracted using the acid–phenol–guanidinium–chloroform (APGC) method as described above after adding 10 mL of the denaturing buffer to the reaction mix. The aqueous layer was precipitated with 2-propanol and resuspended in 1 mL of water, and the extraction/precipitation process was repeated. The final precipitate was resuspended in 1 mL of H_2O. $MgCl_2$ was added to a final concentration of 10 mM and the sample was heated to 75 °C and cooled slowly to room temperature, after which a tyrosine acceptance assay showed the sample to be between 935 and 1050 pmol/A_{260}. The yields from the transcription reaction were 0.9–1.1 mg/mL.

Authentic B. stearothermophilus tRNA^{Tyr}. A sample of crude material was obtained from the Imperial College pilot plant and purified to a tyrosine acceptance of 140 pmol/A_{260}.

Kinetic Techniques. All kinetic studies were performed at 25 ± 0.1 °C in a standard buffer of 144 mM Tris-HCl (pH 7.78), 10 mM $MgCl_2$, 10 mM 2-mercaptoethanol, and 0.1 mM PMSF. All kinetics were analyzed using the Enzfitter nonlinear regression program (Leatherbarrow, 1987).

Steady-State tRNA Charging. The enzyme (2 nM) was preincubated for 5 min with 10 mM Mg·ATP and 100 μM [^{14}C]tyrosine (70 μCi). The substrate tRNA^{Tyr} was added at final concentrations of 0.2–10 μM, and 40-μL aliquots were quenched into 3 mL of 5% TCA after time intervals of 30 s. The quenched samples were filtered through 25-mm nitrocellulose filters prewashed with 5% TCA saturated with cold tyrosine. The filters were dried and counted for ^{14}C in Optiphase "Highsafe" II (LKB) liquid scintillant, twice for 5 min. Initial rates of [^{14}C]Tyr-tRNA formation were plotted against tRNA concentration to enable calculation of the values of k_{cat} for tRNA charging and the K_M for tRNA^{Tyr}. This assay was carried out in triplicate.

Preparation of the Intermediate Tyrosyl Adenylate. The tyrosyl adenylate complex was prepared by incubating the enzyme (10 μM) with 5 mM Mg·ATP (pH 7.0), 20 μM tyrosine, and 1 unit of inorganic pyrophosphatase at 25 °C for 30–45 min. The complex was isolated by gel filtration (Sephadex G25) in 10 mM BisTris (pH 6.0), 10 mM $MgCl_2$, 10 mM 2-mercaptoethanol, and 0.1 mM PMSF. When the complex was prepared for use in quenched-flow experiments, 100% ^{14}C-labeled tyrosine (486 mCi/mmol) was used.

Use of a Stopped-Flow Apparatus To Observe the Reaction with tRNA^{Tyr}. Rate constants for the formation of the complex with tRNA^{Tyr} and the subsequent transition state of tyrosine transfer were obtained by monitoring the protein fluorescence in a stopped-flow spectrophotometer supplied by Applied Photophysics (Model SF 17MV). Excitation was at 285 nm and emission was measured at wavelengths greater than 320 nm using a cutoff filter. The concentration of tyrosyl adenylate complex in one of the syringes was 0.5 μM in 10 mM BisTris (pH 6.0). In the other syringe, tRNA concentrations ranged between 0.5 and 12 μM in 288 mM Tris-HCl (pH 7.78). The stop block of the apparatus was positioned such that 50-μL volumes from each syringe were mixed. The split time-base facility of the stopped-flow was used to observe the tRNA binding and tyrosine transfer phases of the tRNA charging reaction. Progress curves were fitted to exponential equations by using the SF 17MV software package by P. J. King, Applied Photophysics. The rates of the fluorescence changes observed were plotted against tRNA concentration as described later.

Use of a Stopped-Flow Apparatus To Measure the Rate of Product Release. The product of the tyrosyl-tRNA synthetase reaction, Tyr-tRNA, was formed by incubation of the enzyme with 10 mM Mg·ATP, 50 μM tyrosine, and 10 μM *E. coli* tRNA^{Tyr} at 25 °C in 144 mM Tris-HCl, pH 7.78, 10 mM $MgCl_2$, 10 mM 2-mercaptoethanol, and 0.1 mM PMSF. A proportion (5%) of the tyrosine was ^{14}C-labeled to allow determination of the concentration of product obtained. Enzyme and excess substrates were separated from the product by gel filtration using Sephadex G25. In the stopped-flow experiment, the concentration of enzyme in one syringe was 0.5 μM in 144 mM Tris-HCl, pH 7.78, and the concentration of Tyr-tRNA in the other syringe ranged between 0.5 and 10 μM in the same buffer. The stopped-flow apparatus was operated as described in the previous section and the fluorometer was used to observe the binding of Tyr-tRNA to enzyme. The rate of the fluorescence change observed was plotted against tRNA concentration as described later.

Table I: Steady-State tRNA Charging Kinetics[a]

substrate	k_{cat} (s^{-1})	K_M-(tRNA) (μM)	k_{cat}/K_M (s^{-1} M^{-1})
E. coli tRNA^{Tyr} (modified)	3.78 ± 0.15	1.20 ± 0.12	3.15×10^6
B. stearothermophilus tRNA^{Tyr} (modified)[b]	3.70 ± 0.10	1.10 ± 0.10	3.36×10^6
B. stearothermophilus tRNA^{Tyr} (unmodified)[c]	4.00 ± 0.16	1.40 ± 0.22	2.90×10^6
B. stearothermophilus tRNA^{Tyr} (authentic)	3.80[d]		

[a] 25 °C in standard 144 mM Tris-HCl buffer (pH 7.78) with 1.0–2.0 nM TyrRS, 2.5 mM ATP, 100 μM tyrosine, and 0.2–10 μM tRNA^{Tyr}. Rate constants are quoted per mole of dimeric enzyme as measured by active-site titration. Experiments were performed in triplicate. Errors were calculated by the Enzfitter program (Leatherbarrow, 1987). [b] Expressed in *E. coli*. [c] Transcribed in vitro. [d] Wilkinson et al. (1983).

Use of a Pulsed Quenched-Flow Apparatus To Measure the Rate of Tyrosine Transfer to tRNA. A quenched-flow apparatus was used in the pulsed quenched-flow mode (Fersht & Jakes, 1975). The preformed 100% ^{14}C-labeled tyrosyl adenylate complex was in one syringe in 10 mM BisTris (pH 6.0) and 10 mM $MgCl_2$, and a saturating concentration of in vitro-transcribed *B. stearothermophilus* tRNA^{Tyr} (12 μM) in 288 mM Tris-HCl (pH 7.78), 10 mM $MgCl_2$, and 500 μM cold tyrosine was in the other syringe. Time courses of the reaction were constructed (20–180 ms) by mixing, quenching with 10% TCA, collecting the precipitate on nitrocellulose filters, and assaying the [^{14}C]Tyr-tRNA by scintillation counting. Similar experiments were performed with authentic *B. stearothermophilus* tRNA^{Tyr} in which the adenylate was preformed by incubating with 15 μM ^{14}C-labeled tyrosine, 2 mM ATP, 10 mM $MgCl_2$, and 0.1 unit/mL inorganic pyrophosphatase in 144 mM Tris-HCl buffer (pH 7.78).

Measurement of Fluorescence Changes after Binding tRNA^{Tyr} Substrates to TyrRS at Equilibrium. The two substrates used in this experiment were modified *E. coli* tRNA^{Tyr} and unmodified *B. stearothermophilus* tRNA^{Tyr}. tRNA was added to a solution of TyrRS such that the final concentrations of each were 0.5–10.0 μM and 0.5 μM, respectively. Excitation was at 290 nm, and emission scans were recorded between 300 and 500 nm (Perkin Elmer LS50 luminescence spectrometer). Under these conditions, the wavelength of maximum emission of a solution of TyrRS (λ_{max}) is 342–344 nm. Heterogenous yeast RNA (Sigma) was added to solutions of TyrRS at concentrations equivalent to the tRNA^{Tyr} substrates in terms of absorbance at 290 nm as a control to allow for the absorbance of tRNA^{Tyr} at this wavelength (inner filter effect). The changes in fluorescence intensity (ΔF) at each concentration of tRNA were measured and normalized to that of the control RNA to allow for the inner filter effect as discussed later.

RESULTS

Steady-State Charging Kinetics of Modified and Unmodified tRNA^{Tyr} Substrates. Table I compares the steady-state kinetic parameters for the charging of native *E. coli* tRNA^{Tyr}, *B. stearothermophilus* tRNA^{Tyr} expressed in *E. coli*, and in vitro-transcribed *B. stearothermophilus* tRNA^{Tyr}. The values of k_{cat} and K_M are essentially identical for all three tRNA^{Tyr} molecules.

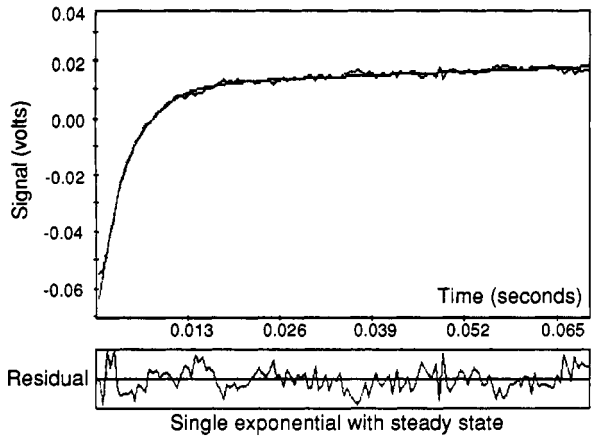

FIGURE 1: Typical trace for change in fluorescence observed upon binding the modified *E. coli* tRNA^{Tyr} and *B. stearothermophilus* tRNA^{Tyr} (expressed in *E. coli*) substrates to tyrosyl-tRNA synthetase in a stopped-flow apparatus (25 °C, 0.25 μM TyrRS, 0.25–6.0 μM tRNA^{Tyr}, 144 mM Tris-HCl, pH 7.78, and 10 mM $MgCl_2$). The trace records an increase in the signal voltage which is equivalent to a decrease in the fluorescence signal (F). The trace is fitted to an exponential equation as described in the text. The accuracy of the fit is indicated by the residual ($F_{obs} - F_{calc}$).

A Fluorescence Change Associated with the Binding of in Vivo Expressed tRNA^{Tyr} Substrates to TyrRS Can Be Observed in a Stopped-Flow Apparatus. Figure 1 shows a typical single-exponential fluorescence decrease (recorded as a signal voltage increase) observed upon mixing either native *E. coli* tRNA^{Tyr} or *B. stearothermophilus* tRNA^{Tyr} with TyrRS in a stopped-flow apparatus in the absence of tyrosine or ATP substrates. There is a 15–20% decrease in protein fluorescence. The rate constant observed for this change increases with increasing tRNA concentrations. This rate is denoted as k_{1obs}.

Scheme I

$$E + tRNA \underset{k_{off}}{\overset{k_{on}}{\rightleftharpoons}} E\cdot tRNA$$

Assuming conditions are such that the enzyme and substrate rapidly equilibrate with their complex (Scheme I), then k_{1obs} follows the relationship

$$k_{1obs} = k_{off} + k_{on}[tRNA] \quad (3)$$

The values of k_{off}, k_{on}, and K_{tRNA} (since $K_{tRNA} = k_{off}/k_{on}$) for the binding of modified tRNA^{Tyr} substrates to TryRS may, therefore, be obtained from plots of k_{1obs} against tRNA concentration (Figure 2). Where the tRNA concentrations used were comparable to enzyme levels, the free concentration of tRNA^{Tyr} was corrected for the proportion of tRNA bound to the enzyme. The results are summarized in Table II. The values of k_{on} for the binding of tRNA to the enzyme are close to diffusion-controlled. The values of K_{tRNA} obtained for the two modified tRNA^{Tyr} substrates are essentially identical.

Native E. coli tRNA^{Tyr} and B. stearothermophilus tRNA^{Tyr}, Expressed in E. coli (Both Modified Substrates), Show Two Fluorescence Changes upon Addition to the E·Tyr-AMP Intermediate. In order to study the pre-steady-state kinetics of step II of the TyrRS reaction by fluorescence, changes must occur upon mixing of the tRNA^{Tyr} with the tyrosyl adenylate intermediate (E·Tyr-AMP). Figure 3 shows the typical fluorescence traces observed in the stopped-flow experiment. Two major fluorescence changes occur. An exponential decrease in fluorescence (recorded as an increase in signal voltage) due to fast binding is followed by a second slower fluorescence change that has an increase in fluorescence. The rate constant for the fluorescence change associated with tRNA binding is again denoted as k_{1obs}. The second change is not seen when tRNA^{Tyr} is added to enzyme alone and, therefore, could be due either to a conformational change associated with the transfer of tyrosine to the tRNA or to product release. The observed rate of this exponential fluorescence change is denoted as k_{2obs}.

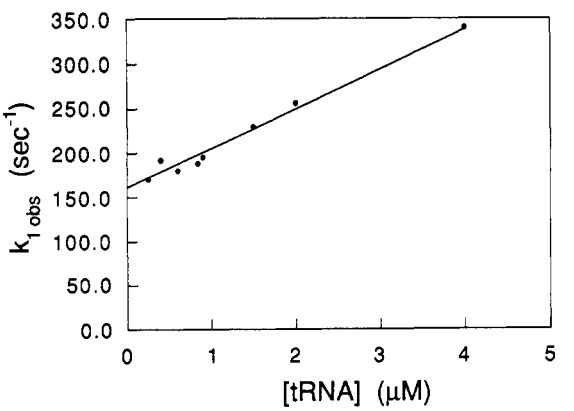

FIGURE 2: Relationship between k_{1obs} and [tRNA] upon binding the modified *E. coli* tRNA^{Tyr} (native) substrate to free TyrRS. k_{1obs} is the rate of binding observed by stopped-flow. Experimental conditions are as described in Table II.

Table II: Rate and Equilibrium Constants for Binding of Modified tRNA^{Tyr} Substrates to Free TyrRS[a]

	k_{on} (s^{-1} M^{-1}) × 10^{-7}	k_{off} (s^{-1})	K_{tRNA}[b] (μM)
E. coli tRNA^{Tyr}	4.57 ± 0.5	158 ± 10	3.46 ± 0.3
B. stearothermophilis tRNA^{Tyr} [c]	5.35 ± 0.5	166 ± 11	3.10 ± 0.5

[a] 25 °C in standard 144 mM Tris-HCl buffer (pH 7.78) with 0.25 μM enzyme and 0.25–5.0 μM tRNA (final concentrations). Fluorescence curves were fitted to exponential equations as described in the text. When [tRNA] is comparable to [enzyme], the free [tRNA] is corrected for the proportion of tRNA bound to the enzyme. Absolute rate and dissociation constants were determined using eq 3. Errors were calculated by the Enzfitter program (Leatherbarrow, 1987). [b] $K_{tRNA} = k_{off}/k_{on}$. [c] Expressed in *E. coli*.

Assuming the tyrosyl-tRNA synthetase reaction proceeds according to Scheme II, the observed rate constant for the second fluorescence change, k_{2obs}, can be related to the concentration of tRNA such that values of k_4, the rate constant for tyrosine transfer, and K_{tRNA}, the dissociation constant of tRNA from the E·Tyr-AMP complex, can be extracted.

Scheme II

$$E\cdot T\text{-}A + tRNA \underset{k_{off}}{\overset{k_{on}}{\rightleftharpoons}} E\cdot T\text{-}A\cdot tRNA \underset{k_{-4}}{\overset{k_4}{\rightleftharpoons}} E\cdot T\text{-}tRNA\cdot A \xrightarrow{k_5} E + T\text{-}tRNA$$

When $k_{off} \gg k_4$, the value of k_{2obs} is related to the concentration of tRNA by eq 4, which is analogous to the Michaelis-Menten equation:

$$k_{2obs} = \frac{k_4[tRNA]}{K_{tRNA} + [tRNA]} \quad (4)$$

Values of k_4 and K_{tRNA} were obtained from fitting the data to the above equation (Figure 4A). However, in the tyrosyl-tRNA synthetase reaction it appears that k_{off} is *not* considerably larger than k_4, and although eq 4 gives a reliable value of k_4, the value of K_{tRNA} obtained is too high by 25–30%.

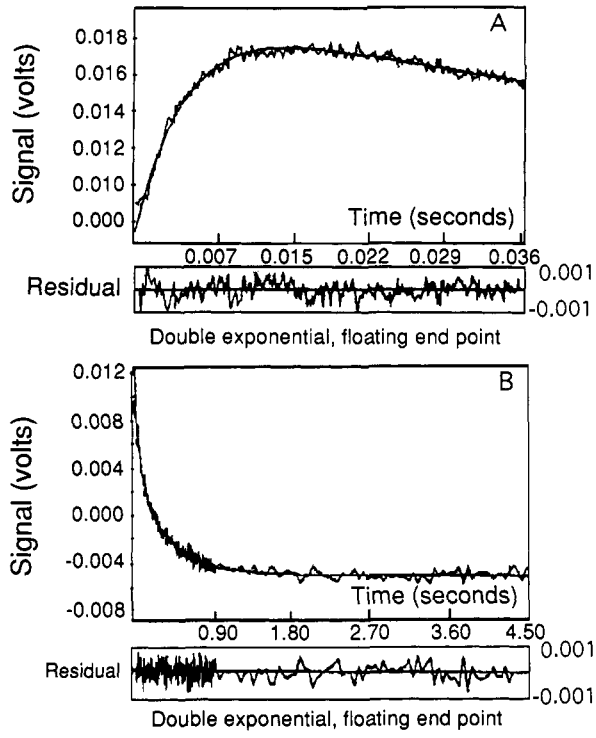

FIGURE 3: Typical fluorescence traces recorded by the stopped-flow spectrophotometer upon mixing equal volumes of 0.25–5.0 μM modified $tRNA^{Tyr}$ substrate (native *E. coli* $tRNA^{Tyr}$ and *B. stearothermophilus* $tRNA^{Tyr}$ expressed in *E. coli*) and E·Tyr-AMP (0.25 μM) under standard conditions (see Figure 1). The traces are fitted to exponential equations as described in the text. (A) Fluorescence change associated with tRNA binding occurring at the observed rate, k_{1obs}. (B) Fluorescence change associated with the tyrosine transfer process occurring at the observed rate, k_{2obs}.

In Scheme II, assuming k_{-4} is negligible, the rate constants mix to give two composite rate constants:

$$k_{1obs} = \{k_{on}[tRNA] + k_{off} + k_4 + [(k_{on}[tRNA] + k_{off} + k_4)^2 - 4k_{on}[tRNA]k_4]^{1/2}\}/2 \quad (5)$$

$$k_{2obs} = \{k_{on}[tRNA] + k_{off} + k_4 - [(k_{on}[tRNA] + k_{off} + k_4)^2 - 4k_{on}[tRNA]k_4]^{1/2}\}/2 \quad (6)$$

Both eqs 4 and 6 give the same value of k_4 since k_{2obs} tends to k_4 as [tRNA] tends to infinity. The simplest way of analyzing the data, however, is to sum eqs 5 and 6 (Fersht & Jencks, 1970; Fersht, 1985) to give

$$k_{1obs} + k_{2obs} = k_{on}[tRNA] + k_{off} + k_4 \quad (7)$$

A plot of $k_{1obs} + k_{2obs}$ against the tRNA concentration (Figure 4B) gives k_{on} from the slope. The value of k_{off} is obtained from the intercept, substituting in the value of k_4 obtained from eq 4 (28.6 s^{-1} and 30.9 s^{-1}, respectively, for the *E. coli* and *B. stearothermophilus* $tRNA^{Tyr}$ substrates). The values of k_4, k_{on}, k_{off}, and K_{tRNA} (since $K_{tRNA} = k_{off}/k_{on}$) obtained for the two modified $tRNA^{Tyr}$ substrates are essentially identical (Table III). The modified $tRNA^{Tyr}$ substrates bind 2–3 times more tightly to TyrRS when tyrosine and ATP are also present at the active site, the difference in K_{tRNA} being a reflection of a decrease in k_{off} (see Tables II and III). This would be expected since transfer of tyrosine to the hydroxyl of the 3′-terminal adenosine of the tRNA subsequently occurs at the active site.

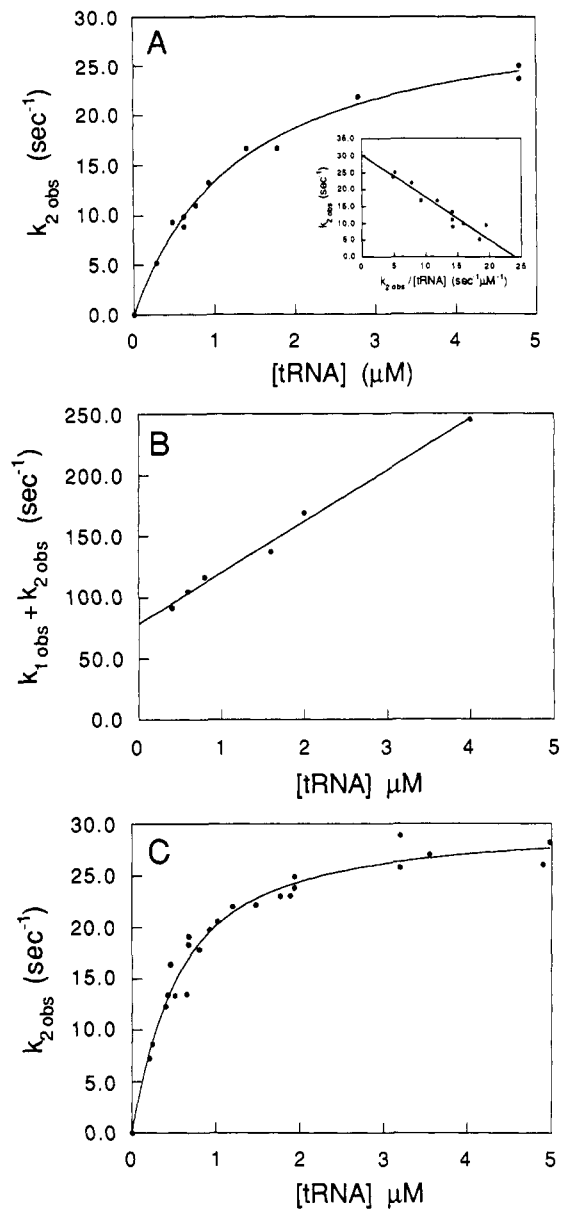

FIGURE 4: Relationship between k_{2obs} and [tRNA], where k_{2obs} is the observed rate of tyrosine transfer from E·Tyr-AMP to $tRNA^{Tyr}$ measured by stopped-flow under conditions described in Figure 3. (A) Typical data for tyrosine transfer to native *E. coli* $tRNA^{Tyr}$ and to *B. stearothermophilus* $tRNA^{Tyr}$ expressed in *E. coli*. Data were fitted to eq 4 as described in the text. The inset is the Eadie–Hofstee transformation of the data. (B) Typical data for tRNA binding and tyrosine transfer to native *E. coli* $tRNA^{Tyr}$ and to *B. stearothermophilus* $tRNA^{Tyr}$ expressed in *E. coli*. The data are fitted to eq 7 as described in the text. (C) Typical data for tyrosine transfer to in vitro-transcribed *B. stearothermophilus* $tRNA^{Tyr}$. The data are fitted to eq 6 as described in the text.

Unmodified $tRNA^{Tyr}$ (B. stearothermophilus) Shows Only the Second Fluorescence Curve Associated with Tyrosine Transfer When Added to E·Tyr-AMP. No fluorescence changes are seen upon mixing this $tRNA^{Tyr}$ with enzyme only. The value of k_{2obs} for this $tRNA^{Tyr}$ substrate was plotted against tRNA concentration as described in the previous section, using eq 4 to obtain the value of k_4 (Table III). The rate constant for tyrosine transfer, k_4, is 30 s^{-1}, a value almost identical to that obtained for the modified $tRNA^{Tyr}$ substrates. Since the first fluorescence change is not observed, eq 7 cannot be used to obtain k_{on}, k_{off}, and K_{tRNA} ($K_{tRNA} = k_{off}/k_{on}$). The data generated using this substrate, therefore, are fitted to eq

Table III: Pre-Steady-State Kinetic Parameters for Tyrosine Transfer Obtained upon Mixing Modified and Unmodified tRNA^{Tyr} Substrates with Adenylate Complex[a]

substrate	k_4 (s^{-1})	K_{tRNA} (μM)	k_{on} (s^{-1} M^{-1}) × 10^{-6}	k_{off} (s^{-1})
E. coli tRNA^{Tyr}	28.6 ± 1.3	1.1 ± 0.10	42.0 ● 2	48.5 ± 4
B. stearothermophilus tRNA^{Tyr} [b]	30.9 ± 1.1	1.2 ± 0.14	50.6 ± 3	57.0 ± 7
B. stearothermophilus tRNA^{Tyr} (unmodified)[c]	30.0 ± 0.2	0.43 ± 0.09	120± 40	52.0 ± 10

[a] Conditions as in Table II, with 0.25 μM adenylate complex and 0.25–5.0 μM tRNA (final concentrations). Absolute rate and dissociation constants calculated by fitting the data to eqs 4, 6, and 7 as described in the text, using the Enzfitter nonlinear regression program. [b] Expressed in *E. coli*. [c] Transcribed in vitro.

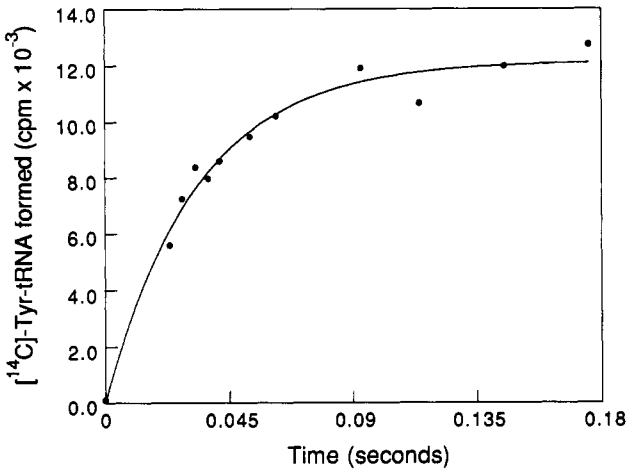

FIGURE 5: Time course for tyrosine transfer to unmodified in vitro-transcribed *B. stearothermophilus* tRNA. Measurements were made using quenched-flow techniques (25 °C, 144 mM Tris-HCl (pH 7.78), 10 mM $MgCl_2$, 0.25 μM E·[^{14}C]Tyr-AMP, and 12 μM tRNA^{Tyr}). The percentage transfer of tyrosine to tRNA was 60%. The data are fitted to a first-order exponential equation.

6, with the value of k_4 fixed at 30 s^{-1} to reduce the error calculated by the Enzfitter program (Leatherbarrow, 1987) on the values of k_{on} and k_{off}. The results are shown in Table III.

The value of K_{tRNA} obtained from the fluorescence change associated with tyrosine transfer is about 2 times lower than that obtained using the fully modified substrates. As binding could be detected for the modified *B. stearothermophilus* tRNA^{Tyr}, expressed in *E. coli*, the different behavior exhibited by the in vitro-transcribed *B. stearothermophilus* tRNA^{Tyr} is not due to its sequence but rather to its lack of modified bases.

The Second Fluorescence Change Observed in Stopped-Flow Occurs with the Same Rate Constant as That Obtained from Pre-Steady-State Quenched-Flow Experiments. When 0.5 μM adenylate complex was mixed with a saturating concentration of in vitro-transcribed tRNA^{Tyr} (12 μM), the [^{14}C]tyrosine is transferred to the tRNA at a rate of 30 ± 2 s^{-1} (Figure 5). The decrease in fluorescence observed in stopped-flow experiments using the same tRNA substrate has a rate constant of 30.0 ± 0.2 s^{-1}, which is identical within experimental error (Table III). Since the quenched-flow experiment is designed to measure specifically the rate of tyrosine transfer, the second fluorescence change observed in the stopped-flow experiment can now be definitely assigned to this step of the reaction. The rate constant from quenched-flow experiments with authentic *B. stearothermophilus* tRNA^{Tyr} is 40 ± 5 s^{-1}.

Measurement of the Rate of Product Release. The rate of the fluorescence change observed upon mixing isolated, preformed product, Tyr-tRNA, with free enzyme in a stopped-flow apparatus fit the relationship described by eq 3, replacing [tRNA] with [Tyr-tRNA], where k_{off} is equivalent to k_5 in Scheme II. The value of k_5, the rate constant for the release of product, could therefore be obtained. This value was calculated as 95 ± 10 s^{-1}. The data confirm that product release is not the rate-determining step in the TyrRS reaction.

Equilibrium Binding Fluorescence Experiments Show No Significant Fluorescence Change upon Binding of Unmodified tRNA^{Tyr} to TyrRS; Modified (E. coli) tRNA^{Tyr} Shows a Fluorescence Decrease and a Red Shift of the Emission Maximum. The lack of detection of binding of the in vitro-transcribed tRNA^{Tyr} does not imply a large difference in binding kinetics; there may be an undetectable change in fluorescence upon binding. This was investigated by fluorescence titration experiments with the modified *E. coli* substrate and the in vitro-transcribed *B. stearothermophilus* tRNA^{Tyr}.

The modified *E. coli* tRNA^{Tyr} and the *B. stearothermophilus* tRNA^{Tyr} transcript were bound to TyrRS in the absence of tyrosine and ATP at equivalent concentrations in terms of tyrosine accepting ability and absorbance. In order to eliminate the inner filter effect, the changes in fluorescence caused by the tRNA substrates were normalized to that of a control sample of RNA which was added at the same absorbance and has little specific binding ability:

$$\Delta F_{norm} = \frac{F_{contol} - F_{sample}}{F_{control}} \quad (8)$$

If binding causes a fluorescence change, then the data should fit eq 9 and enable a value for K_{tRNA} to be determined:

$$\Delta F_{norm} = 1 - K_{tRNA}\Delta F_{norm}/[tRNA] \quad (9)$$

For the modified *E. coli* tRNA^{Tyr} substrate, up to 50% fluorescence quenching was observed, the emission profile broadened, and the emission peak shifted by 10–12 nm to a longer wavelength (Figure 6B). The data produced a reasonable plot (Figure 6A) from which a dissociation constant of 4.5 ± 1.2 μM was obtained. Considering the lower accuracy of this method, the result is in fair agreement with the value of K_{tRNA} obtained by mixing this substrate with TyrRS in a stopped-flow apparatus (3.5 ± 0.3 μM). Upon adding increasing amounts of the in vitro-transcribed tRNA^{Tyr} to TyrRS, the fluorescence decreases proportionately. The linear relationship suggests the fluorescence change is due to the inner filter effect alone and there is little or no effect on protein fluorescence caused by binding of the tRNA transcript.

Calculation of the Energy Levels of the Complex with tRNA and the Subsequent Transition State of Tyrosine Transfer. The free energies of each species up to the intermediate E·Tyr-AMP complex have been previously calculated for catalysis by this enzyme (Fersht, 1987). In this present study, the results obtained using the in vitro-transcribed tRNA^{Tyr} were used to extend the free energy profile for the two-step reaction (Figure 7). Energy levels are calculated relative to $G_{E\cdot Tyr\text{-}AMP}$ using the thermodynamic equations below. The standard state is 1 M for all substrates.

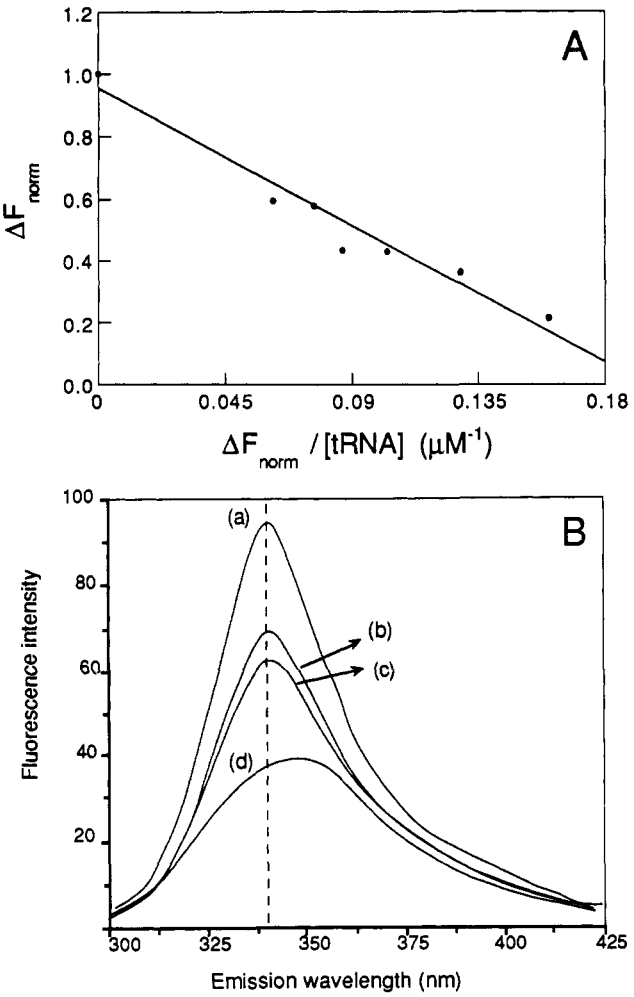

FIGURE 6: Binding of $tRNA^{Tyr}$ substrates to free TyrRS at equilibrium [25 °C, 144 mM Tris (pH 7.78), and 10 mM $MgCl_2$]. (A) Plot of ΔF_{norm} versus ΔF_{norm}/[tRNA] for the binding of *E. coli* $tRNA^{Tyr}$ to free enzyme at equilibrium. (B) Fluorescence emission scans recorded upon binding the following substrates: (a) no substrate, (b) control heterogeneous RNA, (c) in vitro-transcribed *B. stearothermophilus* $tRNA^{Tyr}$, and (d) native *E. coli* $tRNA^{Tyr}$. The ligands (0.5–10.0 μM) have been added to a 0.5 μM solution of TyrRS at equal concentrations in terms of absorbance (see text).

For the binding of tRNA to the adenylate complex:

$$G_{E\cdot T\text{-}A\cdot tRNA} = RT \ln K_{tRNA} \quad (10)$$

For formation of the transition state of the tyrosine transfer step (from transition state theory and $\Delta G_T^{\ddagger} = \Delta G^{\ddagger} + \Delta G_S$ as shown in Figure 7):

$$G_{[E\cdot T\text{-}tRNA\cdot A]^{\ddagger}} = RT \ln (k_B T/h) - RT \ln (k_4/K_{tRNA}) \quad (11)$$

where R is the gas constant, T is the absolute temperature, k_B is Boltzmann's constant, and h is Planck's constant. The enzyme-bound species are as follows: T = tyrosine, A = ATP (or AMP), $[T\text{-}A]^{\ddagger}$ = the transition state of tyrosine activation, T-A = tyrosyl adenylate, PP_i = pyrophosphate, and $[T\text{-}tRNA\cdot A]^{\ddagger}$ = the transition state of tyrosine transfer.

The free energy of the E·Tyr-AMP complex relative to free enzyme is –6.0 kcal mol^{-1} (Wells & Fersht, 1986). The Gibbs' free energies calculated for the two further species on the TyrRS reaction pathway, relative to free enzyme (taking $G_E = 0$), are $G_{E\cdot T\text{-}A\cdot tRNA} = -14.7 \pm 0.01$ kcal mol^{-1} and $G_{[E\cdot T\text{-}tRNA\cdot A]^{\ddagger}} = 0.76 \pm 0.01$ kcal mol^{-1}.

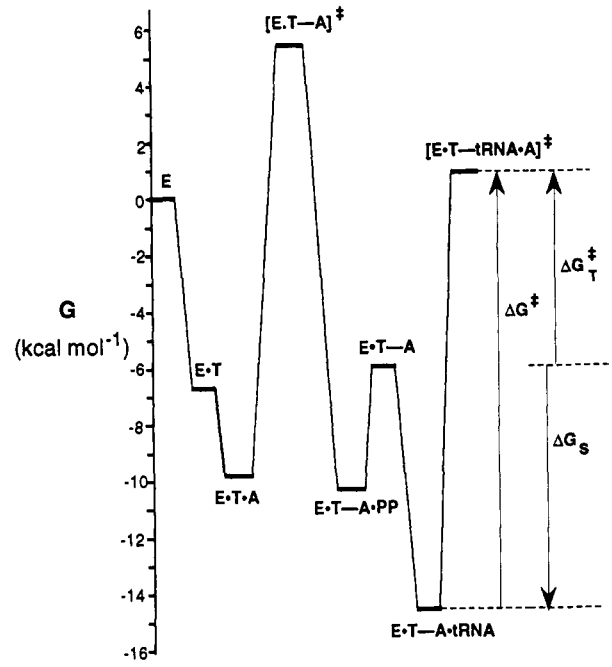

FIGURE 7: Gibbs' free energy profile for catalysis by wild-type tyrosyl-tRNA synthetase extended to include part of the tRNA charging step. The reaction species are defined in the text. ΔG_S, $\Delta G^{\ddagger}$, and $\Delta G_T^{\ddagger}$ represent the substrate binding, activation, and transition-state energies, respectively, during the tyrosine transfer reaction. The standard state is 1 M for all substrates.

DISCUSSION

The steady-state kinetic parameters for charging of *E. coli* $tRNA^{Tyr}$, *B. stearothermophilus* $tRNA^{Tyr}$ expressed in *E. coli*, and *B. stearothermophilus* $tRNA^{Tyr}$ transcribed in vitro are the same, strongly suggesting that neither the species of origin nor the presence of modified bases in the tRNA is important in the kinetics of overall aminoacylation by TyrRS. The effects on individual rate constants have been investigated by studying the individual steps on the reaction pathway by pre-steady-state kinetics. Upon mixing tRNA with free enzyme and/or E·Tyr-AMP, a series of fluorescence changes are observed.

The First Fluorescence Change Is Associated with tRNA Binding. Corroboration of this assignment was provided by equilibrium binding studies. The value of K_{tRNA} obtained using this method is 4.5 ± 1.2 μM, which is in fair agreement with that obtained from the ratio of rate constants for binding and dissociation determined by stopped-flow (3.5 ± 0.3 μM, see Table II). Hence, when the modified $tRNA^{Tyr}$ substrates bind to TyrRS (either the free enzyme or the E·Tyr-AMP complex), protein fluorescence is quenched and the process can be monitored in a stopped-flow apparatus.

The Second Fluorescence Change Is Associated with Tyrosine Transfer to the Bound tRNA. This fluorescence change is observed only when tRNA is mixed with TyrRS in the presence of tyrosine and ATP. The rate constant for this change is 30.0 ± 0.2 s^{-1}. The quenched-flow experiment, designed to measure specifically the rate of tyrosine transfer to $tRNA^{Tyr}$, produces an identical rate constant (30 ± 2 s^{-1}). The quenched-flow experiment, therefore, demonstrates that the second fluorescence change observed in the stopped-flow experiment is concomitant with transfer. Both the tRNA binding and tyrosine transfer processes have, therefore, associated fluorescence changes when the fully modified in vivo-expressed substrates are mixed with E·Tyr-AMP, making step II of the TyrRS reaction amenable to stopped-flow kinetic

analysis. Analysis of the forward reaction has allowed determination of accurate values of k_4 (the rate of tyrosine transfer) and K_{tRNA} for catalysis by wild-type TyrRS. The stopped-flow technique has been used to compare the recognition of different $tRNA^{Tyr}$ substrates by TyrRS.

Comparison of $tRNA^{Tyr}$ Substrates. The pre-steady-state kinetic data have allowed detailed comparison between native *E. coli* $tRNA^{Tyr}$, *B. stearothermophilus* $tRNA^{Tyr}$ expressed in *E. coli*, and in vitro-transcribed *B. stearothermophilus* $tRNA^{Tyr}$ as substrates in the TyrRS reaction. The conclusion drawn from the data in Tables II and III is that all three substrates are kinetically equivalent in the experimental conditions used, as suggested by the steady-state data (Table I).

The Sequence Differences between the Modified E. coli and B. stearothermophilus $tRNA^{Tyr}$ Substrates Are Not in Regions That Are Critical for Specific Recognition by TyrRS. The two tRNA species are recognized equally by TyrRS. The sequences of the two substrates share 72% identity, of which 27% are the nucleotides that are invariant or semi-invariant in all tRNA molecules (Sprinzl & Gauss, 1982). Most of the differences that occur between the two sequences are in the variable loop and D-stem regions. This suggests that these regions are not involved in specific interactions with TyrRS. There are, however, some nucleotides within the D-loop that are the same in both $tRNA^{Tyr}$ sequences and could interact specifically with the enzyme. These observations support the general hypothesis proposed for the binding of tRNA to a class I aminoacyl-tRNA synthetase; that is, that the substrate molecule approaches on the side of its D-loop rather than its variable loop (Ruff et al., 1991). The discriminator base, A73, in the acceptor stem is so far the only residue for which a specific recognition of the base has been clearly demonstrated (Celis & Piper, 1982; Himeno et al., 1990). Previous studies have implicated the anticodon of *E. coli* $tRNA^{Tyr}$ as being important in the recognition process (Ghysen & Celis, 1974; Himeno et al., 1990; Hou & Schimmel, 1989a). It is interesting that the sequences of *E. coli* and *B. stearothermophilus* $tRNA^{Tyr}$ differ by only one base pair in the acceptor stem region (position 70). It also seems likely that the anticodon loop contacts TyrRS as there are no sequence differences between the two $tRNA^{Tyr}$ molecules in this region.

Use of Unmodified in Vitro-Transcribed $tRNA^{Tyr}$ (B. stearothermophilus) Simplifies the Kinetic Analysis of the Tyrosine Transfer Step. The rate of tyrosine transfer to the unmodified in vitro-transcribed $tRNA^{Tyr}$ substrate catalyzed by TyrRS is 30 s^{-1} (Table III), a value essentially identical to that found for the modified $tRNA^{Tyr}$ substrates. However, the value of K_{tRNA} for this substrate appears to be 2–3-fold lower. Addition of the in vitro-transcribed $tRNA^{Tyr}$ substrate to E·Tyr-AMP gives only the fluorescence change associated with tyrosine transfer. The lack of detection of a fluorescence change upon binding of this substrate could be due to changes in the binding kinetics that also produce the lower value for K_{tRNA}. However, the stopped-flow experimental observations do not support a significantly large change in k_{on} or k_{off}, and binding may simply be undetected because there is not a concomitant change in fluorescence. There is strong evidence favouring this alternative, found from changes in fluorescence in equilibrium binding experiments. Addition of the fully modified $tRNA^{Tyr}$ substrate to TyrRS causes a specific effect on protein fluorescence upon binding (Figure 6). The emission peak is broadened and shifts to a longer wavelength. In equivalent experiments using the in vitro-transcribed $tRNA^{Tyr}$, no specific effect on protein fluorescence upon binding of the substrate was observed. This result strongly suggests that the binding of in vitro $tRNA^{Tyr}$ is not detected in a stopped-flow apparatus because it does not cause a fluorescence change. The absence of a fluorescence decrease due to tRNA binding allows more accurate curve fitting of the fluorescence increase associated with tyrosine transfer.

The reason the binding of in vitro-transcribed $tRNA^{Tyr}$ does not have a specific effect on protein fluorescence is presumably that there are no base modifications. One or more of the modified bases present in the in vivo-expressed substrates are probably responsible for affecting the fluorescence properties of a tryptophan in TyrRS. Possible candidates are queuosine, Q, and 2-(methylthio)-N^6-isopentenyladenosine, 2MSI6A, (Sprinzl & Gauss, 1982). The Q is a modification of guanosine and has an additional, partially unsaturated, five-membered ring. The modified base, 2MSI6A, possesses additional unsaturation that could affect tryptophan fluorescence. The effect on fluorescence could be caused by either contact or long-range energy transfer. Alternatively, it is possible that there is an indirect effect on the fluorescence of a tryptophan in TyrRS due to a conformational change caused by binding of the modified $tRNA^{Tyr}$ substrates. The Q and 2MSI6A bases are again the most likely candidates for causing such an effect since they possess the more bulky side chains on their base structures. It is interesting that both these modified bases are in the region of the anticodon loop, thus suggesting this loop may contact TyrRS.

These studies have shown that, under the experimental conditions used, the $tRNA^{Tyr}$ base modifications are not essential for recognition of $tRNA^{Tyr}$ by *B. stearothermophilus* TyrRS. It is convenient that the in vitro-transcribed *B. stearothermophilus* $tRNA^{Tyr}$ substrate gives the most accurate results and is also the easiest to obtain in high amounts and high purity. It should be noted that the in vitro transcript requires denaturing and refolding in the presence of Mg^{2+} before attaining full tyrosine accepting activity, an indication that modified bases do play a role in stabilizing the correct conformation of $tRNA^{Tyr}$, and it is unlikely that an unmodified substrate would be kinetically equivalent in vivo.

Comparison of the Steady-State and Pre-Steady-State Kinetic Data. There is apparent disagreement between the k_{cat}/K_M value of 3.2 μM^{-1} s^{-1} from steady-state studies and k_4/K_{tRNA} of 25–60 μM^{-1} s^{-1} from the pre-steady-state studies presented in this paper. The kinetics of steady-state tRNA charging by TyrRS, like those of many other aminoacyl-tRNA synthetases, are complicated because they are biphasic with respect to tyrosine concentration (Jakes & Fersht, 1975; Wilkinson et al., 1983). It appears that, in the steady state, at high concentrations of tyrosine a second mole of tyrosine binds and enhances the rate by as much as 5-fold. There is better agreement between the steady-state and pre-steady-state kinetic parameters if much higher concentrations of tyrosine are used. The pre-steady-state kinetics, however, involve direct measurements of the individual steps and so are less complicated and easier to interpret.

The Free Energy Profile. The pre-steady-state kinetic data obtained using the in vitro-transcribed tRNA transcript as substrate were used to calculate the free energy levels of two enzyme-bound reaction species along step II of the TyrRS reaction. These are the complex with bound tRNA (E·Tyr-AMP·tRNA) and the transition state of the tyrosine transfer reaction ([E·Tyr-tRNA·AMP]*). Hence, part of the free energy profile for step II can be constructed and joined to that previously calculated for step I of the TyrRS reaction, as

shown in Figure 7 (the TyrRS reaction energy profile cannot yet be completed as the K_{diss} for AMP has not been measured). The enzyme–substrate complex is stabilized by 8.7 kcal mol^{-1} relative to the preceding enzyme-bound reaction species, the E·Tyr-AMP complex, and by 14.7 kcal mol^{-1} relative to free enzyme, E. The term $\Delta G^{\ddagger}$ in Figure 7 represents the free energy barrier for tyrosine transfer to occur. Complementary interactions between the enzyme and the transition state will serve to reduce the magnitude of the second transition-state energy barrier. There may also be a residue at the active site which contributes to reducing this energy barrier by general base catalysis. Residues of TyrRS involved in tRNA binding and/or tyrosine transfer can be identified by protein engineering experiments. To pursue this course, we now have a working system in which the reaction between the intermediate E·Tyr-AMP complex and in vitro-transcribed *B. stearothermophilus* $tRNA^{Tyr}$ can be observed by stopped-flow and absolute rate and dissociation constants can be extracted. The contribution of active-site residues to the tRNA charging reaction in addition to the tyrosine activation step can now be determined. Such experiments have been initiated with particular regard to the mechanisms by which the enzyme optimizes overall catalysis. Interestingly, observation of the free energy profile (Figure 7) shows that the energy barriers to the respective transition states of the two catalytic steps are equal (15.4 kcal mol^{-1}). Optimization of overall catalysis during evolution has probably involved alteration of the free energy profile for both steps of the TyrRS reaction.

REFERENCES

Barker, D. G., Bruton, C. J., & Winter, G. (1982) *FEBS Lett. 150*, 419–423.

Bedouelle, H. (1990) *Biochimie 72*, 589–598.

Bedouelle, H., & Winter, G. (1986) *Nature (London) 320*, 371–373.

Bjork, G. R., Ericson, J. U., Gustafsson, C. E. D., Hagervall, T. G., Jonsson, Y. H., & Wikström, P. M. (1987) *Annu. Rev. Biochem. 56*, 263–287.

Brick, P., & Blow, D. M. (1987) *J. Mol. Biol. 194*, 287–297.

Brick, P., Bhat, T. N., & Blow, D. M. (1989) *J. Mol. Biol. 208*, 83–98.

Burbaum, J. J., & Schimmel, P. (1991) *J. Biol. Chem. 266*, 16965–16968.

Campbell, I. D., & Dwek, R. A. (1984) in *Biological Spectroscopy*, pp 99–126, Benjamin-Cummings, Menlo Park.

Carter, P., Bedouelle, H., & Winter, G. (1986) *Proc. Natl. Acad. Sci. U.S.A. 83*, 1189–1192.

Celis, J. E., & Piper, P. W. (1982) *Nucleic Acids Res. 10*, r83–r91.

Chomczynski, P., & Sacchi, N. (1987) *Anal. Biochem. 162*, 156–159.

Fersht, A. R. (1985) *Enzyme Structure and Mechanism*, W. H. Freeman & Co., San Francisco, CA, and Oxford, England.

Fersht, A. R. (1987) *Biochemistry 26*, 8031–8037.

Fersht, A. R., & Jencks, W. P. (1970) *J. Am. Chem. Soc. 92*, 5432–5442.

Fersht, A. R., & Jakes, R. (1975) *Biochemistry 14*, 3350–3356.

Fersht, A. R., Knill-Jones, J., Bedouelle, H., & Winter, G. (1988) *Biochemistry 27*, 1581–1587.

Ghosh, G., Pelka, H., & Schulman, L. H. (1990) *Biochemistry 29*, 2220–2225.

Ghysen, A., & Celis, J. E. (1974) *J. Mol. Biol. 83*, 333–351.

Grodberg, J., & Dunn, J. J. (1988) *J. Bacteriol. 170*, 1245–1253.

Hall, K. B., Sampson, J. R., Uhlenbeck, O. C., & Redfield, A. (1989) *Biochemistry 28*, 5794–5807.

Hill, K., & Schimmel, P. (1989) *Biochemistry 28*, 2577–2586.

Himeno, H., Hasegawa, T., Ueda, T., Watanabe, K., & Shimizu, M. (1990) *Nucleic Acids Res. 18*, 6815–6819.

Hou, Y.-M., & Schimmel, P. (1989a) *Biochemistry 28*, 4842–4947.

Hou, Y.-M., & Schimmel, P. (1989b) *Nature (London) 337*, 478–481.

Jakes, R., & Fersht, A. R. (1975) *Biochemistry 14*, 3344–3350.

Jones, M. D., Lowe, D. M., Borgford, T., & Fersht, A. R. (1986) *Biochemistry 25*, 1887–1891.

Kim, S.-H., Quigley, G. J., Suddath, F. L., McPherson, A., Sneden, D., Kim, J. J., Weinzierl, J., & Rich, A. (1973) *Science 179*, 285–288.

Labouze, E., & Bedouelle, H. (1989) *J. Mol. Biol. 205*, 729–735.

Leatherbarrow, R. J. (1987) Enzfitter, Elseiver Biosoft, Hills Road, Cambridge, England.

Meinnel, T., Mechulam, Y., Dardel, F., Schmitter, J. M., Hountondji, C., Brunie, S., Dessen, P., Fayat, G., & Blanquet, S. (1990) *Biochimie 72*, 625–632.

Moras, D., Comarmond, M. B., Fischer, J., Weiss, R., Thierry, J. C., Ebel, J.-P., & Giegé, R. (1980) *Nature (London) 288*, 669–674.

Muramatsu, T., Nishikawa, K., Nemoto, F., Kuchino, Y., Nishimura, S., Miyazawa, T., & Yokoyama, S. (1988) *Nature (London) 336*, 179–181.

Normanly, J., & Abelson, J. (1989) *Annu. Rev. Biochem. 58*, 1029–1049.

Perret, V., Garcia, A., Puglisi, J., Grosjean, H., Ebel, J.-P., Florentz, C., & Giegé, R. (1990) *Biochimie 72*, 735–743.

Rossman, M. G., Moras, D., & Olsen, K. W. (1974) *Nature (London) 250*, 194–199.

Ruff, M., Krishnaswamy, S., Boeglin, M., Poterszman, A., Mitschler, A., Podjarny, A., Rees, B., Thierry, J. C., & Moras, D. (1991) *Science 252*, 1682–1689.

Saiki, R. K., Gefan, D. H., Stoffel, S., Scharf, S. J., Higushi, R., Horn, G. T., Mullis, K. B., & Erlich, H. A. (1988) *Science 239*, 487–491.

Sampson, J. R., DiRenzo, A. B., Behlen, L. S., & Uhlenbeck, O. C. (1989) *Science 243*, 1363–1366.

Schimmel, P. (1987) *Annu. Rev. Biochem. 56*, 125–158.

Schimmel, P. (1991) *Trends Biochem. Sci. 16*, 1–3.

Schulman, L. H., & Pelka, H. (1988) *Science 242*, 765–768.

Sprinzl, M., & Gauss, D. H. (1982) *Nucleic Acids Res. 10*, r1–r55.

Stryer, L. (1968) *Science 162*, 526–533.

Stryer, L. (1978) *Annu. Rev. Biochem. 47*, 819–846.

Sussman, J. L., Holbrook, S. R., Wade Warrant, P., Church, G. M., & Kim, S.-H. (1978) *J. Mol. Biol. 123*, 607–630.

Walter, P., Gangloff, J., Bonnet, J., Boulanger, Y., Ebel, J.-P., & Fasiolo, F. (1983) *Proc. Natl. Acad. Sci. U.S.A. 80*, 2437–2441.

Wells, T. N. C., & Fersht, A. R. (1986) *Biochemistry 25*, 1881–1886.

Wells, T. N. C., Knill-Jones, J. W., Gray, T. E., & Fersht, A. R. (1991) *Biochemistry 30*, 5151–5156.

Wilkinson, A. J., Fersht, A. R., Blow, D. M., & Winter, G. (1983) *Biochemistry 22*, 3581–3586.

Woo, N. H., Roe, B. A., & Rich, A. (1980) *Nature (London) 286*, 346–351.